Bioorganic & Medicinal Chemistry 19 (2011) 826–835

Contents lists available at ScienceDirect

Bioorganic & Medicinal Chemistry

journal homepage: www.elsevier.com/locate/bmc

Towards echinomycin mimetics by grafting quinoxaline residues on glycophane scaffolds

Dilip V. Jarikote [a,‡], Wei Li [b,c,†,‡], Tao Jiang [c], Leif A. Eriksson [a,d], Paul V. Murphy [a,*]

[a] School of Chemistry, National University of Ireland, Galway, Ireland
[b] School of Chemistry and Chemical Biology, Centre for Synthesis and Chemical Biology, University College Dublin, Belfield, Dublin 4, Ireland
[c] Key Laboratory of Marine Drugs, The Ministry of Education of China, School of Pharmacy, Ocean University of China, Qingdao 266003, China
[d] School of Science and Technology, Örebro University, 701 82 Örebro, Sweden

ARTICLE INFO

Article history:
Received 9 September 2010
Revised 23 November 2010
Accepted 3 December 2010
Available online 13 December 2010

Keywords:
Echinomycin
Peptidomimetics
Macrocycle
Scaffold
Carbohydrate
DNA

ABSTRACT

Echinomycin is a natural depsipeptide, which is a bisintercalator, inserting quinoxaline units preferentially adjacent to CG base pairs of DNA. Herein the design and synthesis of echinomycin mimetics based on grafting of two quinoxaline residues onto a macrocyclic scaffold (glycophane) is addressed. Binding of the compounds to calf-thymus DNA was studied using UV–vis and steady state fluorescence spectroscopy, as well as thermal denaturation. An interesting observation was enhancement of fluorescence emission for the peptidomimetics on binding to DNA, which contrasted with observations for echinomycin. Molecular dynamics simulations were exploited to explore in more detail if bis-intercalation to DNA was possible for one of the glycophanes. Bis-intercalating echinomycin complexes with DNA were found to be stable during 20 ns simulations at 298 K. However, the MD simulations of a glycophane complexed with a DNA octamer displayed very different behaviour to echinomycin and its quinoxaline units were found to rapidly migrate out from the intercalation site. Release of bis-intercalation strain occurred with only one of the quinoxaline chromophores remaining intercalated throughout the simulation. The distance between the quinoxaline residues in the glycophane at the end of the MD simulation was 7.3–7.5 Å, whereas in echinomycin, the distance between the residues was ~11 Å, suggesting that longer glycophane scaffolds would be required to generate bis-intercalating echinomycin mimetics.

1. Introduction

A number of approaches aimed at regulation of biological processes at the level of the gene are currently being investigated. These include the development of proteins that can inhibit the expression of target genes[1] or the use of RNA interference (RNAi) applied at the post-transcriptional level.[2] There are potential problems with biological approaches in that the bioavailability and delivery of such agents, proteins or nucleic acids can be barriers to their development into useful therapeutics. Proteins and RNAi can also be expensive. Small molecules, prepared by synthetic chemistry, that modulate protein–protein or protein–DNA interactions offer an alterative approach. The polyamides developed by Dervan and co-workers, for example, are DNA-binding small molecules[3] and have been shown to disrupt protein–DNA interactions in a sequence-selective manner.[4] Screening small-molecule and natural product libraries have led to the identification of potential drug candidates in this area. Echinomycin, a natural depsipeptide,[5] described as the prototype bisintercalator,[6] which can insert two quinoxaline units adjacent to CG base pairs of DNA as shown by X-ray crystallography,[7] binds to a sequence recognised by hypoxia inducible factor-1 (HIF-1), known as the hypoxia-responsive element (HRE) which contains the core sequence 5′-(A/G)CGTG-3′ and has been recognised as a point for clinical intervention.[8] A related peptide thiocoraline[5] presumably has a similar bis-intercalation mechanism but does not display any sequence selectivity for DNA.[9] Recent work by Melillo and co-workers,[10] suggest that it may be justified to propose a role for echinomycin in treatment of cancer where HIF-1 activity is high.

For these reasons the development of mimetics of echinomycin would be interesting. Our group and others have been active in the design and synthesis of peptidomimetics[11] which incorporate a carbohydrate component.[12,13] These are generally considered to be non-peptide peptidomimetics. Recently we have been involved in developing glycophane scaffolds,[14] which led us to apply these scaffolds as a basis to generate bivalent inhibitors of carbohydrate–protein interactions at cell surfaces.[14i,j] Herein, we describe the synthesis of echinomycin mimetics (Chart 1) where quinoxaline units were grafted to glycophanes as well as a spectroscopic study of the interactions of these compounds with DNA. The work

* Corresponding author. Fax: +353 91 525700.
E-mail address: paul.v.murphy@nuigalway.ie (P.V. Murphy).
† Present address: School of Pharmacy, Jining Medicinal College, Rizhao 276826, China.
‡ These authors contributed equally.

0968-0896/$ - see front matter © 2010 Elsevier Ltd. All rights reserved.
doi:10.1016/j.bmc.2010.12.009

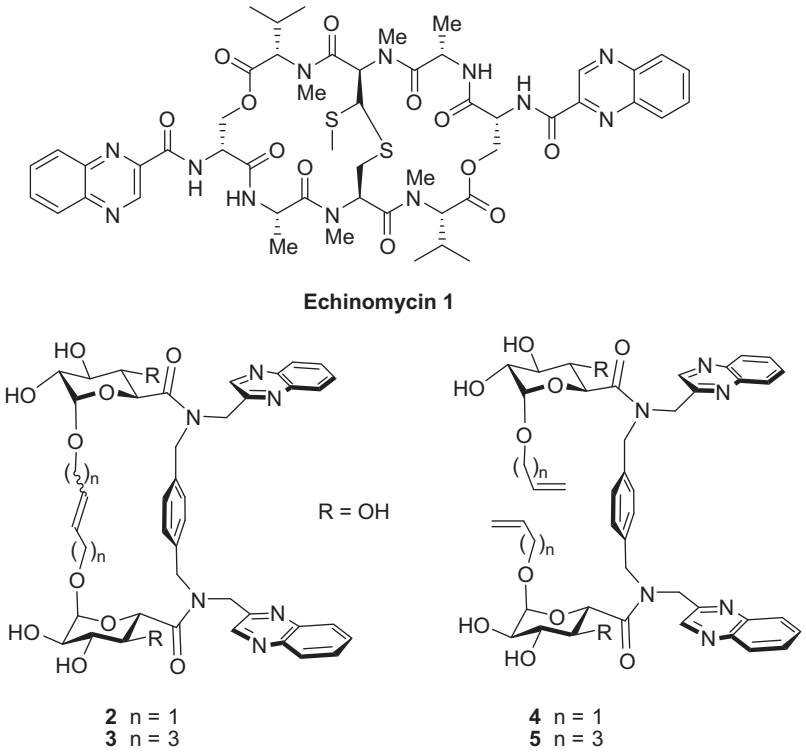

Chart 1. Structures of **1**–**5**.

has provided a basis for development of echinomycin and other depsipeptidomimetics using glycophane and other macrocyclic scaffolds.

2. Results and discussion

2.1. Molecular modelling

The high resolution crystal structure of the bis-intercalation complex of the echinomycin with $(ACGTACGT)_2$ was used for the first computationally based docking experiment. We first wanted to establish whether the placement of the quinoxaline residues onto the glycophane scaffold, such as in **2**, could adopt a similar spacing to that found in echinomycin **1** and potentially intercalate without unfavourable steric interactions to DNA. A model was therefore built using Macromodel (for both *E* and *Z*-isomers) of **2** so that the distance between the quinoxaline residues and their respective orientation matched that found in the X-ray structure of echinomycin complexed to the $(ACGT)_2$ sequence. Next this conformation of **2** was manually docked into the site where echinomycin was located; the quinoxaline residues were placed at identical locations to those adopted by the same residues of echinomycin. The echinomycin residue was then deleted from the model, leaving **2** and then the energy minimization of the complex of **2** with the $(ACGT)_2$ was carried out giving the model shown in Figure 1b. Having shown that **2** had potential to bisintercalate we commenced with its synthesis as well as that of the more flexible analogues such as glycophane **3** and acyclic analogues **4** and **5**.

2.2. Synthesis of echinomycin mimetics

The synthesis of the glycophane derivatives was achieved from glycosides **8** and **9** which were derived from glucuronic acid, as previously described (Scheme 1).[15] Thus the aldehyde **6**[16] was reacted with *p*-xylylenediamine to give a diimine intermediate. Subsequent reduction of the diimine with sodium cyanoborohydride gave the diamine **7**. The reaction of **8/9** with oxalyl chloride gave the respective acid chlorides and their subsequent reaction with **7** gave **10/11**. Ring closure metathesis (RCM) using the Grubbs-I catalyst and subsequent deacetylation gave **2/3**. Both the ^{1}H NMR and ^{13}C NMR spectra of **2** and **3** showed more than one set of signals. For **3** one major alkene isomer (trans isomer) is present and the presence of multiple signal sets is due to the existence of rotamers **3a** and **3b** which result from amide bond isomerisation (Chart 2) and which exchange slowly enough that both isomers can be observed by NMR. Hence for **3a** both amides have *Z*-configuration, whereas for **3b** one amide is *Z* and the other has the *E*-configuration.[17] For **2** two signal sets were also observed. However in this case it is due to the presence of a mixture of both the *cis* (*Z*) and *trans* (*E*) alkene isomers (1:1) from the RCM reaction. There is no amide isomerism observed for **2**. This is because **2** is smaller and significantly more constrained than **3** and isomerisation of the amides from ZZ to EZ in **2** would give rise to a more strained macrocycle. This proposal is supported by conformational analysis carried out using Macromodel[18] which indicates the isomer of **2** with E and Z amides would be ~12 kJ/mol less stable than the isomer where the amides have both E configurations. Efforts to reduce alkene of **2** by catalytic hydrogenation led to reduction of the imine of the quinazoline residue and was not pursued for other compounds. All subsequent biophysical studies with **2** were carried out with the mixture of alkenes, which were not separable using chromatography.

The direct deacetylation of **10/11** gave respectively **4/5**. The presence of multiple signals for **4** and **5** (e.g., δ 100.3, 100.2 and 100.0 for the anomeric carbon for **5** in its ^{13}C NMR spectrum) indicated, similarly to **3**, that **4**/**5** are mixtures of rotamers.

2.3. Spectroscopic based measurements

Obtaining samples of **2–5** provided the opportunity to study their binding or interaction with DNA. Previous binding studies with echinomycin have been carried out using NMR, DSC, CD and

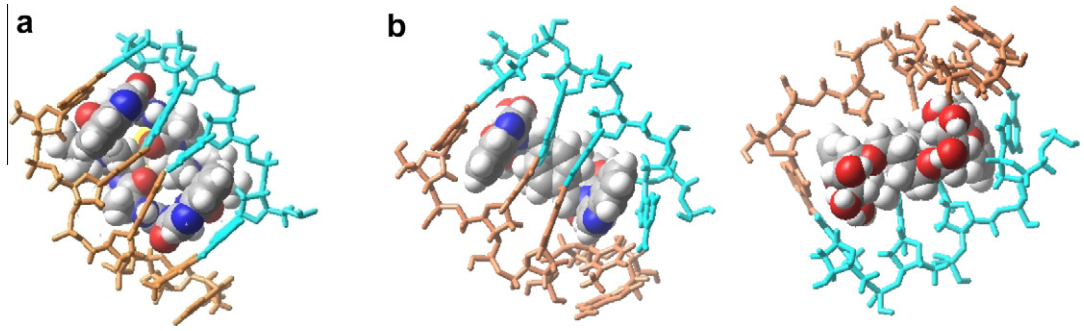

Figure 1. (a) ACGT and echinomycin **1** bound fragment of the X-ray crystal structure of **1** (PDB ID: 2ADW[7]). (b) Two views of the initial model of **2** (trans alkene isomer) docked to ACGT.

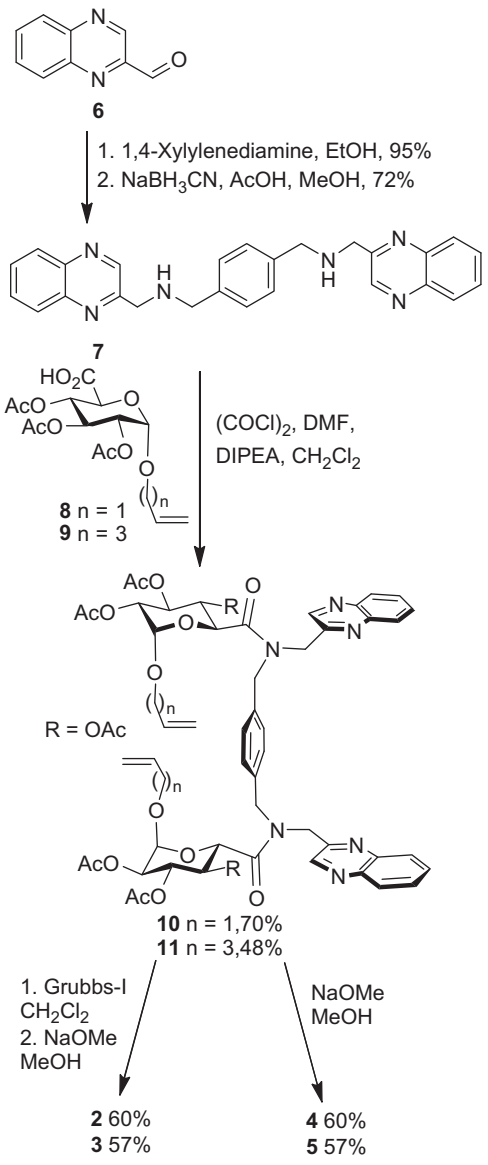

Scheme 1. Synthesis of **2**–**5**.

fluorescence spectroscopy.[19] Herein UV–vis and steady state fluorescence and CD spectroscopy were applied. The thermal denaturation of DNA was also studied in the absence and presence of the compounds.

The effect of adding increasing amounts of DNA on the UV absorbance spectrum of echinomycin (20 μM) in aqueous buffer was first studied. Echinomycin was shown to exist as a monomer before and after binding with calf thymus DNA at the concentrations used as described previously.[20] Addition of calf thymus DNA to the echinomycin solution resulted in a gradual reduction of the intensity of the broad band maximum wavelength (~325 nm) in the absorbance spectra. The UV absorbance spectra[21] of free **2**–**5** were measured and they were found to have extinction coefficients similar to echinomycin itself (Table 1); the absorbance maximum of free **2** (321 nm) and **3** (319 nm) was blue-shifted by 4 and 6 nm, respectively, when compared to the free echinomycin. As for echinomycin, the titration of calf thymus DNA to **2** and **3** caused a gradual decrease of intensity of the absorption band in the visible region of the spectrum. The observed results were consistent with the binding of the chromophores of both echinomycin and the mimetics **2–5** to double stranded DNA.

The properties of quinoxaline chromophores in various compounds upon their interaction with DNA were next explored by steady state fluorescence emission spectroscopy. It has been reported that the fluorescence of echinomycin is gradually quenched upon titration with DNA duplexes.[19f] This observation was replicated during this study (Fig. 2); in order to observe the emission spectrum excitation was carried out at a wavelength of 285 nm and at saturation no further change in fluorescence quenching was recorded. The fluorescence spectra of **2–5** are shown in Figures 3 and 4, respectively, both in absence and presence of increasing concentrations of DNA. Before treatment with DNA, **2** showed a strong fluorescence emission band at 420 and at 351 nm. Interestingly when **2** was titrated with calf-thymus DNA fluorescence enhancement was observed with a 5.5-fold fluorescence enhancement noted at 320 nm. These observations are important as fluorescence enhancement on binding with duplex DNA has previously only been observed with particular intercalators such as thiazole orange derivatives and ethidium bromide.[22]

Untreated acyclic compounds **4** and **5** were strongly fluorescent and were almost 4–5-fold more fluorescent when compared with the more conformationally locked derivatives **2** and **3**. Compounds **4** and **5** showed emission maxima at 370 and 391 nm, respectively. The addition of DNA led to 2.8-fold fluorescence enhancements for both **4** and **5**, respectively. The different spectral shape (compare Figs. 3 and 4) and comparatively low fluorescence enhancement observed for the acyclic compounds may be due to these compounds having a different binding mode to the DNA duplex, possibly due to their flexibility.

The thermal stabilities were next measured for the calf thymus DNA duplex before and after hybridising with **2–5** and echinomycin. The melting temp of calf thymus DNA duplex was recorded (T_M = 76 °C). The melting temp of calf thymus DNA upon binding with **2** (T_M = 78 °C) and **3** (T_M = 79 °C) had increased in both cases. The calf thymus DNA showed high duplex stability upon binding with **4** (T_M = 79 °C) and **5** (T_M = 81 °C) also. The value for echinomy-

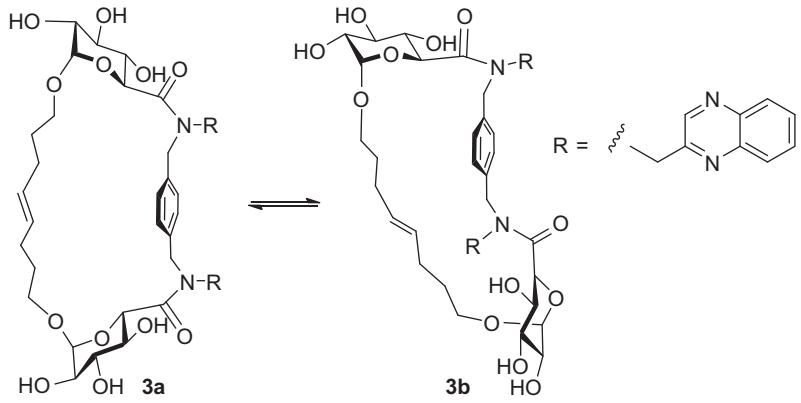

Chart 2. Rotamers of **3**.

Table 1
Spectroscopic parameters of free echinomycin, **2**, **3**, **4** and **5**

Substrate	$\lambda_{max(abs)}$[a] (nm)	ε[b] (M^{-1} cm^{-1})	$\lambda_{max(em)}$[c] (nm)
Echinomycin	325	11,500	387
2	321	10,481	416
3	319	11,126	394
4	320	11,668	369
5	320	12,302	391

[a] Wavelength of absorbance maximum.
[b] Extinction coefficient at absorbance maximum.
[c] Wavelength of fluorescence emission maximum.

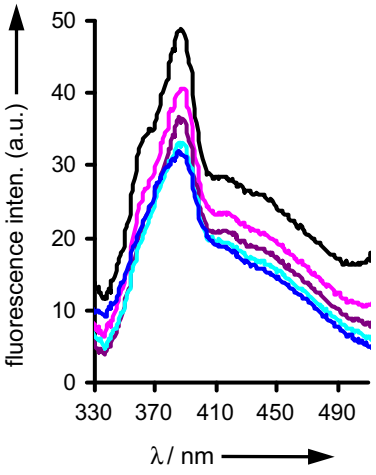

Figure 2. Fluorescence emission spectra of echinomycin **1** before (black) and after addition of calf thymus DNA [2 (pink), 4 (violet), 6 (turquoise) and 8 μM (blue)]. Measurement conditions: 20 μM in degassed buffer (100 mM NaCl, 10 mM NaH_2PO_4 at pH 7.0). Ex. 285 nm, Em. 318–550 nm Ex. Slit: 10 nm and Em. Slit. 10 nm.

cin was T_M = 79 °C. The comparison of the melting temp in the absence and presence of the compounds suggests that **2–5** and echinomycin are binding to the DNA duplex and inducing higher duplex stability. The observed high stability of duplexes is similar with the previously reported binding of daunomycin, cryptolepine and chlorobenzylidine with DNA duplexes.[23]

2.4. Molecular dynamics simulations

The use of computational methods to gain insights into possible modes of binding or interaction of the glycophane based echinomycin derivatives was next explored. Both the bis-intercalation complexes of the $(ACGTACGT)_2$ sequence with two echinomycin molecules (PDB ID: 2ADW[7]), and the corresponding initial model with two glycophane molecules **2** docked in the place of echinomycin, were explored by means of molecular dynamics (MD) simulations. All simulations were performed using the YASARA code,[24] and the Amber03 force field.[25] The DNA–drug complexes were soaked in a water box of approximate dimensions 55 × 31 × 30 Å, containing 1200–1300 TIP3P water molecules giving a total of 5100–5200 atoms. The cell was neutralized by replacing random water molecules by counterions (Na^+) and corrected to an overall ionic strength corresponding to physiological conditions. Following energy minimization based on steepest decent and simulated annealing techniques, three sets of 20 ns MD simulations were conducted for each system (i.e., echinomycin bound to the DNA sequence and **2** bound to the DNA sequence). These included (i) a simulation at 298 K, starting from the energy minimized structure, (ii) a simulation of the same system at T = 150 K, and (iii) a simulation at 298 K starting from the end point of the 20 ns simulation at 150 K. In order to verify the DNA-water system to be stable, a 32 ns MD simulation of the pure DNA octamer system was also conducted at T = 298 K for benchmarking purposes, using the same force fields and neutralization techniques as above. The pure DNA simulations showed the approach to function very well, giving a system with only minor end-effects in that the outmost base pairs to some degree starts to hydrogen bond to the aqueous environment. All simulations were conducted in the NPT ensemble approximation with periodic boundary conditions, and used Particle Mesh Ewald (PME) summation for long-range Coulomb interactions with cutoff at 7.86 Å. The simulations were conducted using 1.25 fs time steps. Intermolecular forces were recalculated every two simulation steps, and pressure control employed to maintain a water density of 1.00 g/cm^3. The simulations showed that the introduction of the bis-interacalating compounds at the minor groove forces a partial unwinding of the DNA double helix. Instead of the 10 base pair long full helix turn in crystalline DNA, the X-ray structure of the echinomycin–DNA octamer complex reveals a mere 1/4 turn rotation in eight base pairs. The reduced coiling is also accompanied by a stretching of the DNA chain, as seen in Figure 5. The same observation is noted for the DNA octamer complexed with two glycophane molecules **2** (Fig. 5). The DNA-echinomycin structure remained very stable throughout each of the 20 ns simulations; in Figure 6 we display the structures of the echinomycin–DNA complexes (energy minimized) before and after the 20 ns MD simulations at 298 K. As seen in the figure, the overall structures are well retained, albeit with some minor end effects in that the terminal base pairs start interacting with and form hydrogen bonds to the surrounding water molecules. The RMSD between the two structures is 2.613 Å over all 782 atoms of the DNA–echi-

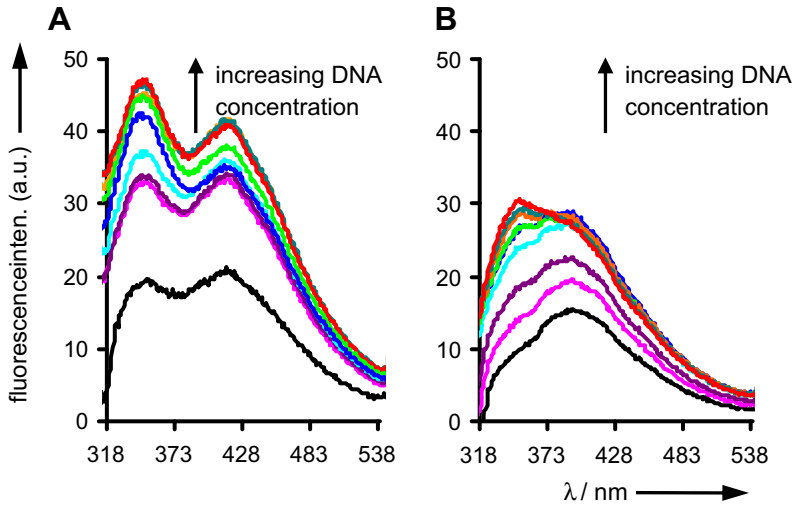

Figure 3. Fluorescence emission spectra of (A) **2** and (B) **3** before (Black) and after addition of calf thymus DNA [2 (pink), 4 (violet), 6 (turquoise), 8 (blue), 10 (bright green), 12 (orange) and 14 (teal), 16 (red), and 18 μM (grey)]. Measurement conditions: see caption of Figure 5.

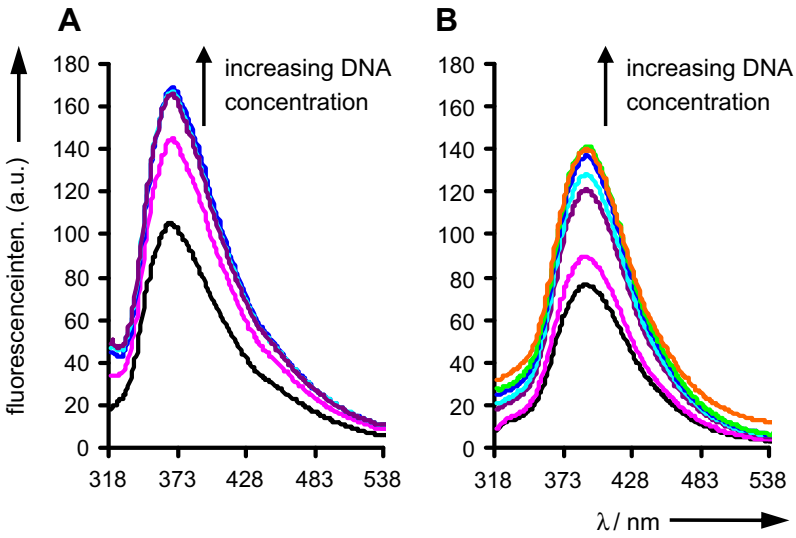

Figure 4. Fluorescence emission spectra of **4** (A) and **5** (B) before (black) and after addition of calf thymus DNA [2 (pink), 4 (violet), 6 (turquoise), 8 (blue), 10 (bright green), 12 (orange) and 14 (teal), 16 (red), and 18 μM (grey)]. Measurement conditions: see caption of Figure 5.

nomycin complex; for the echinomycin moieties alone, the RMSDs are 1.64 and 1.88 Å, respectively. No difference in interactions are noted from the 20 ns at 150 K followed by 20 ns at 298 K simulations, compared with running the simulation for 20 ns at 298 K only.

The MD simulations of compound **2** complexed with the DNA octamer however displayed very different behaviour to that of echinomycin. In the 20 ns simulation at 298 K, several of the quinoxaline units rapidly migrate out from the intercalation sites, and within 5 ns simulation only one of the total four chromophores present at the beginning remained intercalating. Releasing the bis-intercalation strain from the system furthermore allowed the DNA double helix to twist back towards its natural coiled helix structure. The system then remained having only one intercalating unit throughout the simulation (see Fig. 6).

In the case of 20 ns simulation at 150 K, the system is far more stable than at 298 K. One of the two peptidomimetic compounds remains bis-intercalated throughout the simulation, and one is mono-intercalated with the second quinoxaline ring aligned in a 'flat' orientation with the π-system facing the DNA-stack. However, upon heating the system to 298 K for another 20 ns MD simulation, the bis-intercalating entity very rapidly (within 1 ns) attained a mono-intercalated conformation, which was retained for the remainder of the simulation. The main rationale behind the difficulty for glycophane **2** to stay bis-intercalated is to be found in the length of the linker backbone. The distance between the nitrogens connecting the scaffold to the quinoxaline rings is only 7.3–7.5 Å, whereas in echinomycin, the corresponding linker length is approximately 11 Å. Given that the linker length is restricted by the xylylene moiety, which is the same for all four systems synthesized herein, a very similar behaviour can be expected also for compounds 3–**5** (not simulated during this work).

2.5. Summary and conclusions

Glycophane scaffolds to which chromophores are grafted provides a basis for the design compounds that can interact with DNA, as is the case for natural depsipeptide backbones. This extends the applications of glycophanes as scaffolds in bioorganic chemistry, as they can be modified with recognition groups, in this

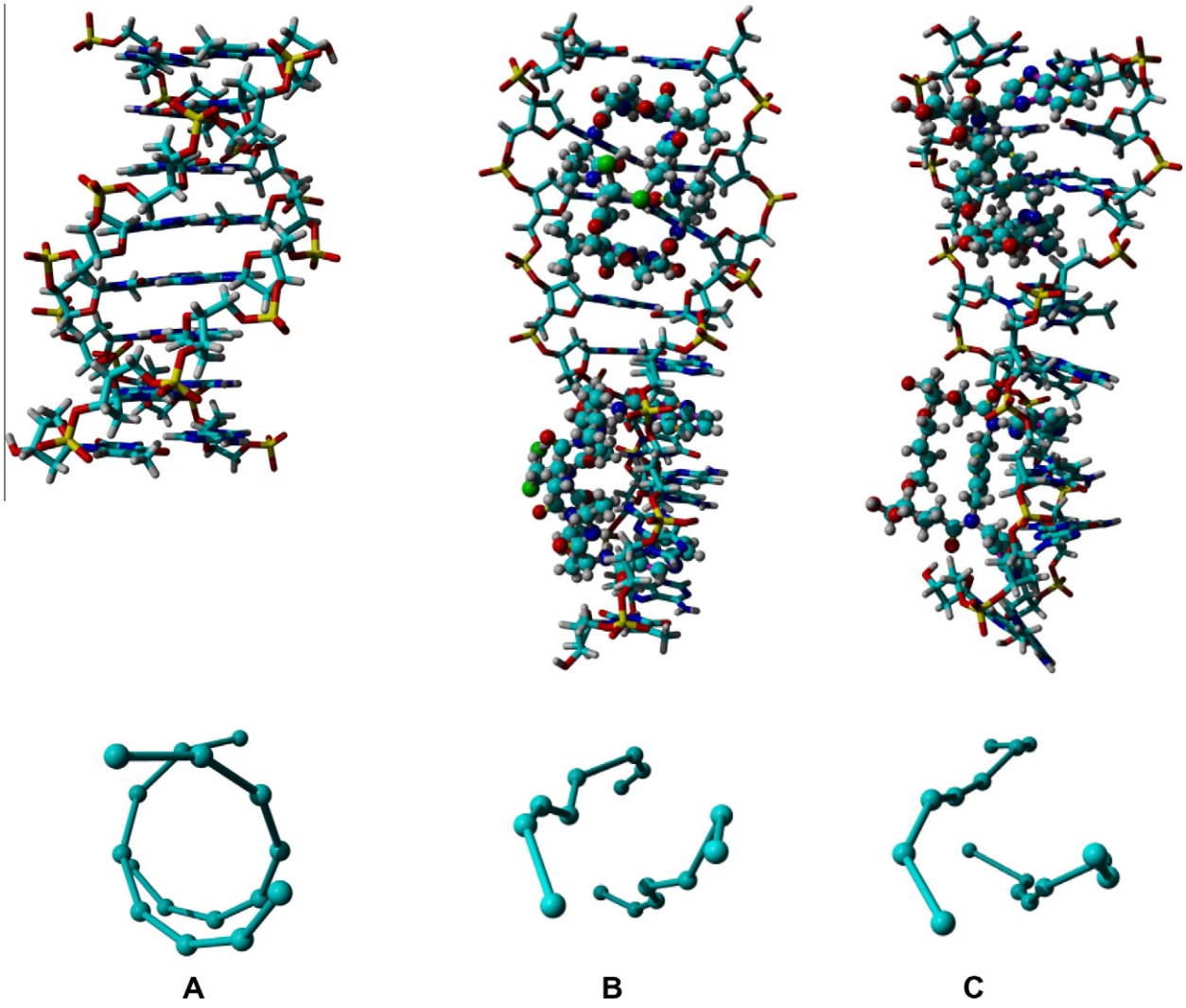

Figure 5. (a) DNA $(ACGTACGT)_2$ octamer. (b) X-ray structure of two echinomycin molecules and (c) model of glycophane molecule **2**, bound to samt DNA octamer. Top row: DNA in stick model, echinomycin/glycophane in ball and stick. Bottom row: top view displaying the reduced coiling of the DNA backbone.

case quinoxaline residues, to give compounds that bind to nucleic acids. Spectroscopic measurements and melting experiments indicated the glycophane derivatives bind to DNA. Molecular dynamics simulations indicated that the glycophanes complex with a DNA octamer in a different manner to echinomycin; whereas echinomycin bis-intercalates the glycophanes derived from *p*-xylylenediamine backbone mono-intercalate. In order to obtain mimetics of echinomycin (i.e., bis-intercalators) glycophanes which have a distance between the residues of ~11 Å would be more optimal. The high affinity of echinomycin for DNA and its sharp sequence selectivity derive from the cyclic peptide portion which fits into the minor groove of DNA, establishing contacts (H-bonds) with DNA. This would also need to be considered in synthesis of mimetics which would have high affinity and selectivity.

3. Experimental section

3.1. General

Optical rotations were determined at the sodium D line at 20 °C. Chemical shifts in NMR spectra are reported relative to internal Me_4Si in $CDCl_3$ (δ 0.0), HOD for D_2O (δ 4.80) for ^1H and $CDCl_3$ (δ 77.0) for ^{13}C at 30 °C, unless otherwise stated ^{13}C signals were assigned with the aid of DEPT-135, HSQC and HMBC. ^1H NMR signals were assigned with the aid of COSY. Coupling constants are reported in Hertz. FTIR spectra were recorded using either thin film between NaCl plates or KBr discs, as specified. Low and high resolution mass spectra were measured on either LC–MS/MS or LC Time-of-flight (LCT) mass spectrometers and were measured in positive and/or negative mode as indicated. TLC was performed on aluminium sheets precoated with silica Gel and spots visualized by UV and charring with H_2SO_4–EtOH (1:20) and/or PMA, $KMnO_4$, ninhydrine or mostaine solutions. Column chromatography was carried out using Silica Gel (0.040–0.630 micron, Merck) and using a stepwise solvent polarity gradient (starting from the conditions indicated in each case and increasing the polarity) correlated with TLC mobility. Reaction solvents were freshly dried and distilled where stated: acetonitrile, toluene and dichloromethane from calcium hydride; MeOH from magnesium turnings and tetrahydrofuran from sodium wire. Alternatively, dichloromethane, tetrahydrofuran and MeOH were used as obtained from a Pure-Solv solvent purification system. Anhydrous DMF and pyridine were used as purchased from Sigma–Aldrich. Molecular sieves are activated 4 Å molecular sieves. Semi-preparative HPLC used reverse phase YMC-Pack ODS-AQ (S5 μm, 250 × 20 mm) unless otherwise stated. The wavelength for detection of peaks using preparative HPLC was 259 nm. All compounds subjected to the biophysical study were purified by semi-preparative HPLC. The fluorescence

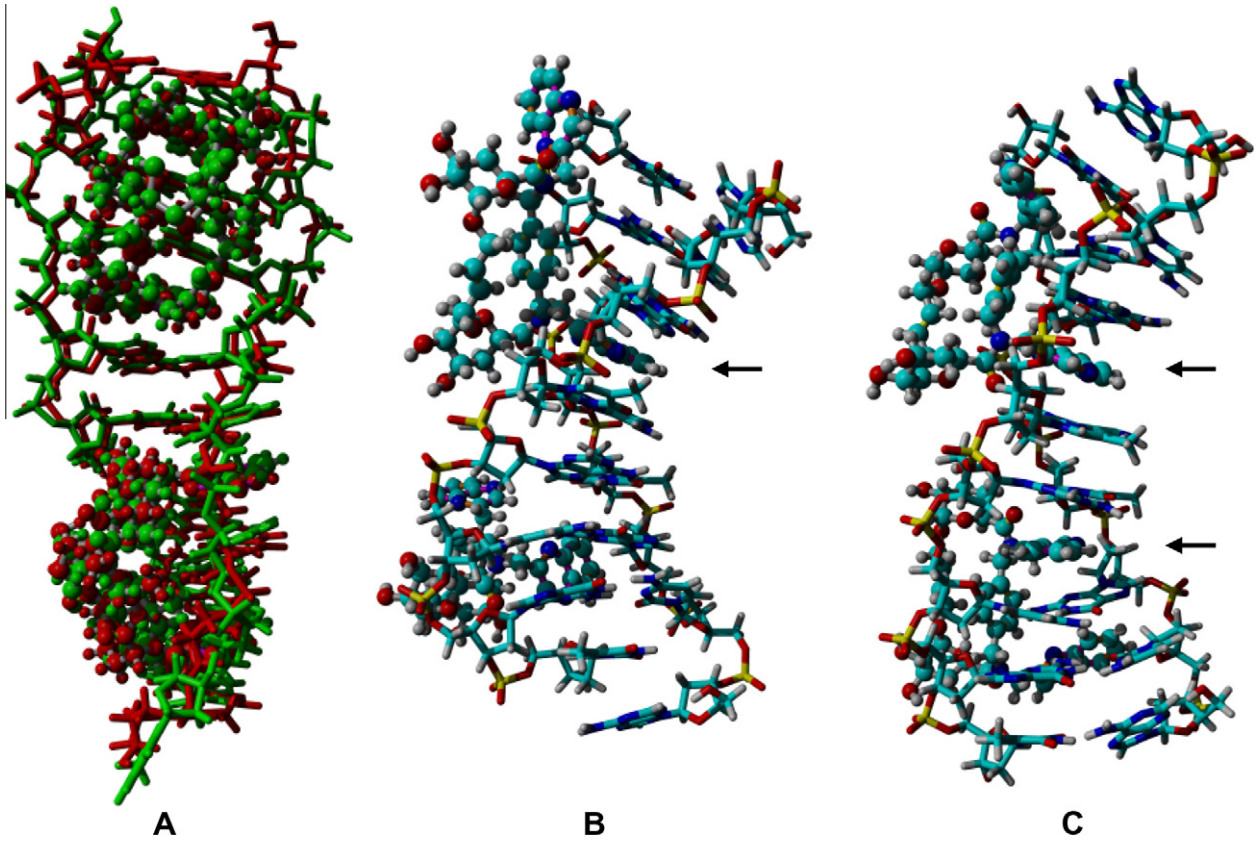

Figure 6. (A) Alignment of DNA octamer complexed with two echinomycin before (green) and after (red) 20 ns simulation at 298 K. (B) DNA octamer with two glycophanes **2**, after 20 ns simulation at 298 K. Intercalating unit indicated by an arrow. (C) As (B), after 20 ns simulation at 150 K, followed by 20 ns simulation at 298 K.

experiments were performed using Varian Cary Eclipse spectrophotometer. A Varian Cary 50 Bio-UV/vis spectrophotometer was used for the optical analysis and a Varian Cary 100 Bio-UV/vis spectrophotometer was used for the thermal denaturation experiments, respectively. Circular-dichroism spectroscopy was carried out using a JASCO 810 CD spectrometer in phosphate buffer at 20 °C. All chemicals and DNA were purchased from Sigma-Aldrich. Water was purified with a Milli-Q® Ultrapure Water Purification System and Millipore Corp. The concentration of DNA solution was determined by using the average extinction coefficient of ε_{260} = 6600 M^{-1} cm^{-1} in water. The echinomycin concentration was determined using the molar extinction coefficient of ε_{325} = 11,500 M^{-1} cm^{-1} in aq buffer.

3.2. Absorbance measurements

The titration experiments were carried out by adding a stock solution of compounds to a fluorescence quartz cuvette and diluted with aq degassed buffer (100 mM NaCl, 10 mM NaH_2PO_4 at pH 7.0) to a final concentration of 20 μM. The absorbance spectrum was recorded at 25 °C. DNA from stock solutions was added as required to obtaining the specified concentration. After each addition the solution was heated at 65 °C and it was cooled to room temp slowly (5 °C/min). After 20 min the spectra were recorded at the specified temp.

3.3. Thermal denaturation study

Melting analysis was carried out using UV spectroscopy. The thermal denaturation was carried out whilst observing changes in absorbance at 260 nm. The buffer solution of 100 mM NaCl, 10 mM NaH_2PO_4 at pH 7.0 was degassed using vacuum. The calf thymus DNA and compounds were then mixed and the solutions adjusted to the final required concentration. The samples were heated to 65 °C and cooled down to 20 °C before commencing the experiment. The samples were then heated to 95 °C at a rate of 1 °C/min. Melting temps (T_M) were defined as the maximum of the first derivative of the melting curve. The T_M values reported in the text are an average of two experiments.

3.4. Fluorescence measurements

The fluorescence experiments were performed with samples previously prepared for absorbance study. The fluorescence measurements were carried out at 25 °C with excitation at 285 nm (excitation slit width: 10 nm; emission slit width: 10 nm). Solvent background signals were subtracted.

3.4.1. *N,N'*-[1,4-Phenylenebis(methylene)]-bis-(1-(quinoxalin-2-yl)methanamine) 7

Quinoxaline-2-carbaldehyde **6**[26] (1.58 g, 10 mmol) was dissolved in EtOH (150 mL) and 1, 4-xylylenediamine (0.63 g, 4.6 mmol) was then added and mixture was stirred at 75 °C for 3 h. The mixture was then cooled to room temp and the precipitate was filtered and washed with EtOH (×3) to give the intermediate diimine as an off-white solid (1.82 g, 95%); mp = 185–186 °C. The diimine (1.81 g, 4.3 mmol) was dissolved in MeOH (50 mL) and then cooled over an ice bath. Sodium cyanoborohydride (273 mg, 4.3 mmol) and acetic acid (4 mL) were added to the cooled solution and the suspended solid dissolved gradually whilst the mixture was stirred at room temp for 3 h. The volatile components were evaporated under diminished pressure. Ethyl acetate was then

added to residue and this was then washed with aq $NaHCO_3$. The aq layer was further extracted with EtOAc (3 × 10 mL). The combined organic layer was dried ($MgSO_4$), filtered and the solvent was removed. Chromatography of the residue (EtOAc–MeOH, 2:1) gave **7** as a dark red solid (1.31 g, 72%); mp = 116–117 °C; ^{1}H NMR ($CDCl_3$, 500 MHz): δ = 8.88 (s, 2H), 8.05-8.09 (m, 4H), 7.70–7.76 (m, 4H), 7.35 (s, 4H), 4.16 (s, 4H), 3.92 (s, 4H), 2.23 (s, 2H, N*H*); ^{13}C NMR (125 MHz, $CDCl_3$) δ 154.9 (C), 145.3, 141.9, 141.8 (each CH), 138.7 (C), 130.0, 129.3, 129.2, 129.0, 128.4 (each CH), 53.4, 52.8 (each CH_2). HRMS (ESI): Found 443.1960 $[M+Na]^+$, $C_{26}H_{24}N_6Na$ requires 443.1968.

3.4.2. *N,N'*-Bis(quinoxalin-2-ylmethyl)-*N,N'*-[1,4-phenylenebis (methylene)]-bis-(allyl 2,3,4,-tri-*O*-acetyl-α-D-glucopyranosiduronamide) 10

The acid **8** (307 mg, 0.79 mmol) was dissolved in dry dichloromethane (10 mL) and then cooled over ice and placed under nitrogen. Dry DMF (100 μL) and oxalyl chloride (100 μL, 1.2 mmol) were then added and the mixture stirred over ice for 15 min and at room temperature for 1 h. The reaction mixture was again cooled over ice and the amine **7** (147 mg, 0.35 mmol) and dry DIPEA (200 μL, 1.14 mmol) in dry dichloromethane (10 mL) were transferred to the flask. The mixture was stirred over ice for 15 min and subsequently at room temp for 15 h. The reaction mixture was then diluted with dichloromethane (10 mL) and washed with HCl (10 mL of 0.1 M) and satd $NaHCO_3$ (10 mL). The aq phase was extracted further with dichloromethane (3 × 10 mL) and the combined extracts were dried ($MgSO_4$), filtered and the solvent was removed under reduced pressure. Chromatography (cyclohexane–EtOAc, 1:3) gave **10** (270 mg, 70%); R_f = 0.34 (cyclohexane–EtOAc, 1:3); mp = 100–102 °C; $[\alpha]_D$ = +56.5 (*c* 1.04, $CHCl_3$); ^{1}H NMR ($CDCl_3$, 400 MHz): δ = 8.82 (br s, 1H), 8.71 and 8.72 (each s, 1H), 8.01–8.14 (m, 4H), 7.73–7.82 (m, 4H), 7.09–7.31 (4H), 5.60–5.74 (m, 2H) overlapping 5.47–5.50 (m, 4H), 5.09–5.16 (m, 4H) overlapping 4.91–5.10 (m, 4H) overlapping 4.77–5.16 (m, 4H) overlapping 4.59–4.78 (m, 4H), 3.94–4.05 (m, 2H) overlapping 3.81–3.96 (m, 2H), 1.90–2.05 (m, 18H); ^{13}C ($CDCl_3$, 100 MHz) δ = 171.1, 170.3, 169.9, 168.7, 167.3 (each CO), 166.9, 166.8 (each NC=O), 151.7, 151.0 (C), 145.3, 143.4 (CH), 141.7, 141.8, 141.9 (each C), 136.3, 135.9, 135.7, 135.2 (C), 132.6, 132.4 (CH), 130.7,130.2, 130.1, 129.7, 129.3, 129.1, 129.0, 128.7, 127.8, 127.5 (each CH), 118.3, 117.9 (CH_2), 95.8, 95.7 70.3 (CH), 69.7 (CH) 69.9 (CH_2), 66.5, 66.7 (each CH), 50.4, 50.2, 49.2, 49.8 (each CH_2), 21.0, 20.7, 20.6 (each $COCH_3$). HRMS (ESI): Found 1105.4046 $[M+H]^+$, $C_{56}H_{61}N_6O_{18}$ requires 1105.4042.

3.4.3. *N,N'*-Bis(quinoxalin-2-ylmethyl)-*N,N'*-[1,4-phenylenebis (methylene)]-bis-(pent-4-enyl 2,3,4,-tri-*O*-acetyl-α-D-glucopyranosiduronamide) 11

Reaction of the acid **9** (582 mg, 1.5 mmol) as described for **8** gave **11** (390 mg, 48%) as a yellow solid; R_f = 0.5 (CH_2Cl_2–EtOAc, 1:2); mp = 84–86 °C; $[\alpha]_D$ = +56.5 (*c* 1.0, $CHCl_3$); ^{1}H NMR ($CDCl_3$, 500 MHz): δ = 8.82 (br s, 1H), 8.72 (br s, 2H), 8.01-8.14 (m, 4H), 7.72–7.83 (m, 4H), 7.09–7.31 (4H), 5.45–5.71 (m, 6H), 5.10 (m, 2H), 4.56–4.95 (m, 16H), 3.22–3.60 (m, 4H), 2.01–2.05 (m, 18H), 1.90–1.91 (m, 4H), 1.49–1.58 (m, 2H), 1.37–1.44 (m, 2H); ^{13}C NMR ($CDCl_3$, 125 MHz) δ = 170.4, 170.0, 169.9, 168.8, 168.7, 167.3, 167.0, 166.9 (each C=O), 151.7, 151.1, 145.3, 143.3 (each C), 142.0, 141.9, 141.7 (each C), 137.3, 137.2 (each CH), 136.3, 135.8, 135.6, 135.1 (each C), 130.7, 130.6, 130.2 130.1, 129.7, 129.4, 129.3, 129.1, 129.0, 128.7, 127.9, 127.5 (each CH), 115.3, 115.1 (each CH_2), 96.7, 96.6, 70.5, 70.0, 69.9, 69.8 (each CH), 69.3, 69.1 (each CH_2), 66.8, 66.7 (each CH), 50.4, 50.2, 49.9, 49.2, 49.1, 48.9, 48.8, 29.8, 29.7, 29.6, 29.5, 28.5, 28.4, 28.3 (each CH_2), 20.7, 20.6, 20.5 (each $COCH_3$). HRMS (ESI): Found 1161.4613 $[M+H]^+$, $C_{60}H_{69}N_6O_{18}$ requires 1161.4668.

3.4.4. *N,N'*-Bis(quinoxalin-2-ylmethyl)-*N,N'*-[1,4-phenylenebis (methylene)]-2-butene-1,4-diyl-bis-α-D-glucopyranosiduronamide 2

A degassed solution of **10** (132 mg, 0.12 mmol) in dry dichloromethane (120 mL, 1 mM) and under argon was treated with Grubbs I catalyst (31 mg, 25%) for 42 h. The solvent was evaporated and chromatography of the residue (dichloromethane–EtOAc, 1:3) gave the protected intermediate (129 mg, 71%) as a grey solid; R_f = 0.15 (dichloromethane–EtOAc, 1:2). To this intermediate (80 mg, 0.074 mmol) in dry methanol (10 mL) and dry dichloromethane (5 mL) that was pre-cooled over ice, sodium methoxide (0.1 mL from a freshly prepared 1 M solution in MeOH) was added and the reaction mixture was stirred at 0 °C for 30 min. The solvent was removed under reduced pressure to give a yellow solid residue. This was dissolved in water and the solution was acidified to pH 6 by addition of amberlite resin (H^+). The resin was removed by filtration and the filtrate was lyophilized to give the macrocyclic product as a white solid (52.2 mg, 85%); $[\alpha]_D$ = +30.0 (*c* 1.07, CH_3OH); ^{1}H NMR ($CDCl_3$, 400 MHz): δ = 8.97 and 8.95 (each s, 2H), 8.05–8.08 (m, 4H), 7.79–7.86 (m, 4H), 7.29 (s, 2H), 7.23 (s, 2H), 5.53 (d, *J* = 15.7 Hz, 1H), 5.45 (t, *J* = 3.4 Hz, 1H), 5.40 (d, *J* = 16.2 Hz, 2H), 5.33 (t, *J* = 3.4 Hz, 1H), 5.22 (d, *J* = 17.5 Hz, 2H), 4.71 (d, *J* = 3.7 Hz, 1H), 4.66–4.69 (m, 2H), 4.53–4.64 (m, 6H), 3.77–3.81 (m, 2H), 3.64–3.72 (m, 8H), 3.50 (dd, *J* = 3.4 Hz and 9.3 Hz, 2H), 3.45 (dd, *J* = 3.7 Hz and 9.7 Hz, 2H); ^{13}C NMR ($CDCl_3$, 100 MHz): δ = 173.4, 162.7 (each CO), 154.1, 153.8 (each C), 146.3, 146.1 (each CH), 143.0, 142.9, 142.7, 137.7, 137.51 (each C), 131.8, 131.8, 131.3, 131.3, 129.9, 129.8, 129.8, 129.80, 129.49, 128.7, 128.1, 128.0, 127.7 (each CH), 100.9, 100.8 (each C), 74.8, 74.5, 73.8, 73.1, 72.9, 69.8, 69.1 (each CH), 69.0, 65.6 (each CH_2) 52.8, 52.5, 52.4, 52.3 (each CH_2); HRMS (ESI): Found 825.3065 $[M+H]^+$, $C_{42}H_{45}N_6O_{12}$ requires 825.3095.

3.4.5. *N,N'*-Bis(quinoxalin-2-ylmethyl)-*N,N'*-[1,4-phenylenebis (methylene)]-4-octene-1,8-diyl-bis-α-D-glucopyranosiduronamide 3

Ring closing metathesis of **11** and subsequent de-*O*-acetylation as described for **10** gave **3** (29 mg, 57%) as an off-white solid; R_f = 0.5 (EtOAc–MeOH, 2:1); mp = 163–165 °C; $[\alpha]_D$ = +15.6 (*c* 1.0, CH_3OH); ^{1}H NMR ($CDCl_3$, 500 MHz): δ = 8.78 and 8.82 (each s, 2H), 8.01–8.04 (m, 4H), 7.70–7.80 (m, 4H), 7.26–7.28 (m, 4H), 5.14–5.16 (m, 1H), 5.08–5.09 (m, 1H), 4.95–4.98 (m, 2H), 4.84–4.86 (m, 2H), 4.68–4.71 (m, 2H), 4.65–4.67 (m, 2H), 4.49 (dd, *J* = 5.4 Hz and 15.6 Hz, 2H), 3.83–3.87 (m, 2H), 3.69–3.75 (m, 2H), 3.59 (dd, *J* = 8.6 and 15.3 Hz, 2H), 3.48–3.53 (m, 2H), 3.40–3.44 (m, 2H), 3.31–3.32 (m, 3H), 1.78–1.84 (m, 2H), 1.66–1.73 (m, 2H), 1.49–1.57 (m, 2H), 1.40–1.47 (m, 2H); ^{13}C (CD_3OD, 125 MHz): δ = 170.5 (C=O), 152.6, 144.7, 141.4, 141.0, 135.7 (each C), 130.2, 129.8, 129.7, 129.5, 129.1, 128.4, 128.3, 127.8, 127.4, 100.2, 72.9, 72.3, 72.1 (each CH), 68.7 (CH_2), 68.3 (CH), 51.2, 49.5, 29.1, 28.6, 23.2 (each CH_2); HRMS (ESI): Found 881.3690 $[M+H]^+$, $C_{46}H_{53}N_6O_{12}$ requires 881.3721.

3.4.6. *N,N'*-Bis(quinoxalin-2-ylmethyl)-*N,N'*-[1,4-phenylenebis (methylene)]-bis-(allyl α-D-glucopyranosiduronamide) 4

De-*O*-acetylation of **10** (59 mg, 0.053 mmol) gave **4** (21 mg, 46%) as an off-white solid; R_f = 0.5 (EtOAc–MeOH, 2:1); ^{1}H NMR ($CDCl_3$, 400 MHz): δ = 8.83 (s, 1H), 8.71 and 8.70 (each s), 8.05–8.08 (m, 4H), 7.79–7.85 (m, 4H), 7.26 (m, 2H), 7.16–7.32 (m, 2H), 5.70–5.77 (m, 2H), 5.53 (d, *J* = 15.7 Hz, 1H) overlapping 5.45 (t, *J* = 3.4 Hz, 1H) overlapping 5.41 (d, *J* = 16.2 Hz, 1H), 5.30–5.36 (m, 2H) overlapping 5.20–5.26 (m, 1H) overlapping 5.09–5.17 (m, 1H), 4.99–5.06 (m, 2H), 4.93–4.97 (m, 1H), 4.53–4.72 (m, 8H), 3.82–3.97 (m, 2H), 3.65–3.81 (m, 6H), 3.44–3.52 (m, 2H); ^{13}C NMR ($CDCl_3$, 100 MHz): δ = 171.4, 170.8 (each amide CO), 152.6, 144.6, 143.7, 141.3, 141.1, 135.8, 135.2, 133.6, 133.1, 130.4,

130.2, 129.9, 129.7, 128.3, 128.0, 127.4, 126.9, 126.2, 116.3, 115.3, 98.9, 98.7, 73.3, 73.0, 72.6, 72.2, 71.6, 68.9, 68.5, 68.2, 67.6, 67.5, 64.2, 51.1, 50.4, 49.9, 49.6. HRMS (ESI): Found 853.3440 $[M+H]^+$, $C_{44}H_{49}N_6O_{12}$ requires 853.3408.

3.4.7. *N,N'*-Bis(quinoxalin-2-ylmethyl)-*N,N'*-[1,4-phenylenebis (methylene)]-bis-(pent-4-enyl α-D-glucopyranosiduronamide) 5

De-*O*-acetylation of **11** gave **5** (23 mg, 49%) as a white solid and as a mixture of *E* and *Z* -isomers, $R_f = 0.5$ (EtOAc–MeOH, 2:1); mp = 118–120 °C; $[\alpha]_D = +8.4$ (*c* 1.0, CH_3OH); ^1H NMR (CD_3OD, 500 MHz): $\delta = 8.83$ (br s, 1H) 8.73 and 8.72 (each s, 1H), 8.02–8.08 (m, 4H), 7.77–7.85 (m, 4H), 7.16–7.32 (m, 4H), 5.62–5.72 (m, 1H), 5.39–5.49 (m, 1H) overlapping 5.28–5.35 (m, 1H), 4.93–5.11 (m, 3H) overlapping 4.83–4.91 (m, 2H) overlapping 4.81–4.83 (m, 4H), 4.75–4.78 (m, 2H), 4.50–4.71 (m, 6H), 3.75–3.84 (m, 2H) overlapping 3.64–3.70 (m, 2H) overlapping 3.34–3.54 (m, 4H), 3.12–3.21 (m, 2H), 1.83–2.02 (m, 2H), 1.61–1.68 (m, 1H), 1.46–1.57 (m, 2H), 1.13–1.16 (m, 2H); ^{13}C (CD_3OD, 125 MHz): $\delta = 171.4$, 170.8 (each C=O), 152.6, 152.1, 144.6, 143.7, 141.5, 141.3, 141.1 (each C), 137.8, 137.5 (each CH), 136.3, 135.8, 135.4 (each C), 130.5, 130.2, 129.9, 129.8, 128.7, 128.5, 128.4, 128.3, 128.1, 127.5, 126.9 (each CH), 114.0, 113.9, 113.6 (each CH_2), 100.0, 99.7, 73.2, 73.0, 72.7, 72.3, 71.7, 71.6, 68.6, 68.5 (each CH), 67.9, 67.8, 51.1, 50.5, 50.3, 49.8, 49.7, 49.6, 29.8, 29.4, 28.4, 28.0 (each CH_2). HRMS (ESI): Found 909.4047 $[M+H]^+$, $C_{48}H_{57}N_6O_{12}$ requires 909.4034.

3.5. Initial molecular modeling docking and minimization

The high resolution crystal structure of the bis-intercalation complex of the echinomycin with $(ACGTACGT)_2$[15] obtained from the Protein Databank (http://www.rcsb.org/pdb/; PDB ID: 2ADW) was used. A fragment of the X-ray structure selected using Macromodel. Thus all atoms were deleted with the exception of an $(ACGT)_2$ fragment complexed to echinomycin. All bonds and hybridizations of atoms were then checked and hydrogen atoms were then added in Macromodel. This led to phosphate residues being converted to phosphonic acids for the purpose of the modelling. A model of **2** (trans isomer) was then built in Macromodel so that distance between the quinoxaline residues projected from the nitrogen atoms of the scaffold and their respective orientation matched that found in the X-ray structure of echinomycin complexed to the $(ACGT)_2$ sequence. Next this structure **2** was manually docked into the site where echinomycin was located using the quinoxaline residues as a guide. Thus the quinoxaline residues of the model of **2** were superimposed so that they were overlayed with identical atoms of the quinoxaline residues of echinomycin. The echinomycin residue was then deleted. Subsequently the complex of **2** and $(ACGT)_2$ which remained was energy minimized to remove any unfavourable interactions that existed from the docking. The OPLSAA force field in Macromodel was applied in the energy minimization. The pdb file of this minimized structure has been included with Supplementary data.

3.6. Molecular dynamics simulations

The bis-intercalation complex of the $(ACGTACGT)_2$ sequence with two Echinomycin molecules (PDB ID 2ADW), and the corresponding model with two glycophane molecules **2** docked in the place of echinomycin, were explored by means of molecular dynamics (MD) simulations. All simulations were performed using the YASARA code,[24] and the Amber03 force field.[25] The DNA–drug complexes were soaked in a water box of approximate dimensions $55 \times 31 \times 30$ Å, containing 1200–1300 TIP3P water molecules giving a total of 5100–5200 atoms. The cell was neutralized by replacing random water molecules by counterions (Na^+) and corrected to an overall ionic strength corresponding to physiological conditions. Following energy minimization based on steepest decent and simulated annealing techniques, sets of 20 ns MD simulations were conducted for each system as described in the main text. All simulations were conducted in the NPT ensemble approximation with periodic boundary conditions, and used Particle Mesh Ewald (PME) summation for long-range Coulomb interactions with cutoff at 7.86 Å. The simulations were conducted using 1.25 fs time steps. Intermolecular forces were recalculated every two simulation steps, and pressure control employed to maintain a water density of 1.00 g/cm^3.

Acknowledgements

The authors are grateful to Science Foundation Ireland (RFP/06/CHEO32), NUI Galway, and the European Commission (Marie Curie EIF Grant No. 220948), the Chinese Ministry of Education and the Chinese Scholarship Council for funding.

Supplementary data

Supplementary data associated with this article can be found, in the online version, at doi:10.1016/j.bmc.2010.12.009.

References and notes

1. Blancafort, P.; Segal, D. J.; Barbas, C. F. *Mol. Pharmacol.* **2004**, *66*, 1361. and cited references.
2. Fire, A.; Xu, S. Q.; Montgomery, M. K.; Kostas, S. A.; Driver, S. E.; Melillo, C. C. *Nature* **1998**, *391*, 806.
3. Dervan, P. B. *Bioorg. Med. Chem.* **2001**, *9*, 2215.
4. Nickols, N. G.; Jacobs, C. S.; Farkas, M. E.; Dervan, P. B. *ACS Chem. Biol.* **2007**, *2*, 561. and cited references.
5. (a) Corbaz, R.; Ettlinger, L.; Gaumann, E.; Keller-Schierlein, W.; Kradolfer, F.; Neipp, L.; Prelog, V.; Reusser, P.; Zahner, H. *Helv. Chim. Acta* **1957**, *40*, 199; (b) Yoshida, T.; Katagiri, K.; Yokozawa, S. *J. Antibiot.* **1961**, *14*, 330.
6. Dawson, S.; Malkinson, J. P.; Paumier, D.; Searcey, M. *Nat. Prod. Rep.* **2007**, *24*, 109.
7. Cuesta-Seijo, J. A.; Sheldrick, G. M. *Acta Crystallogr., Sect. D* **2005**, *61*, 442. and cited references.
8. Cohen, H. T.; McGovern, F. J. *N. Eng. J. Med.* **2005**, *353*, 2477.
9. Boger, D. L.; Ichikawa, S.; Tse, W. C.; Hedrick, M. P.; Jin, Q. *J. Am. Chem. Soc.* **2001**, *123*, 561.
10. Kong, D.; Park, E. J.; Stephen, A. G.; Calvani, M.; Cardellina, J. H.; Monks, A.; Fisher, R. J.; Shoemaker, R. H.; Melillo, G. *Cancer Res.* **2005**, *65*, 9047.
11. For recent reviews on peptidomimetic development see: (a) Robinson, J. A.; DeMarco, S.; Gombert, F.; Moehle, K.; Obrecht, D. *Drug Discovery Today* **2008**, *13*, 944; (b) Clynen, E.; Baggerman, G.; Husson, S. J.; Landuyt, B.; Schoofs, L. *Expert. Opin. Drug Discov.* **2008**, *3*, 425; (c) Vagner, J.; Qu, H. C.; Hruby, V. J. *Curr. Opin. Chem. Biol.* **2008**, *12*, 292.
12. Hirschmann, R.; Nicolaou, K. C.; Pietranico, S.; Leahy, E. M.; Salvino, J.; Arison, B. H.; Cichy, M. A.; Spoors, P. G.; Shakespeare, W. C.; Sprengeler, P. A.; Hamley, P., ; Smith, A. B., III; Reisine, T.; Raynor, K.; Maechler, L.; Donaldson, C.; Vale, W.; Freidinger, R. M.; Cascieri, M. A.; Strader, C. D. *J. Am. Chem. Soc.* **1993**, *115*, 12550.
13. For recent reviews on peptidomimetics derived from carbohydrates see: (a) Murphy, P. V.; Dunne, J. L. *Curr. Org. Synth.* **2006**, *3*, 403; (b) Velter, I.; La Ferla, B.; Nicotra, F. *J. Carbohydr. Chem.* **2006**, *25*, 97; (c) Murphy, P. V. *Eur. J. Org. Chem.* **2007**, 4177; (d) Murphy, P. V.; Velasco-Torrijos, T. In *Glycoscience-Chemistry and Chemical Biology*; Fraser-Reid, B., Tatsuta, K., Thiem, J., Eds., 2nd ed.; Springer: Berlin-Heidelberg, 2008; p 997; (e) Jarikote, D. V.; Murphy, P. V. *Eur. J. Org. Chem.* **2010**, 4959.
14. For synthesis and application of glycophanes, see: (a) Bukownik, R. R.; Wilcox, C. S. *J. Org. Chem.* **1988**, *53*, 463; (b) Jimenez-Barbero, J.; Junquera, E.; Martin-Pastor, M.; Sharma, S.; Vicent, C.; Penades, S. J. *J. Am. Chem. Soc.* **1995**, *117*, 11198; (c) Savage, P. B.; William, D.; Dalley, N. K. *J. Inclusion Phenom. Mol. Recognit. Chem.* **1997**, *29*, 335; (d) Morales, J. C.; Penades, S. *Angew. Chem., Int. Ed.* **1998**, *37*, 654; (e) Belghiti, T.; Joly, J.-P.; Didierjean, C.; Dahaoui, S.; Chapleur, Y. *Tetrahedron Lett.* **2002**, *43*, 1441; (f) Leyden, R.; Murphy, P. V. *Synlett* **2009**, 1949; (g) Velasco-Torrijos, T.; Murphy, P. V. *Org. Lett.* **2004**, *6*, 3961; (h) Velasco-Torrijos, T.; Murphy, P. V. *Tetrahedron: Asymmetry* **2005**, *16*, 261; (i) André, S.; Velasco-Torrijos, T.; Leyden, R.; Gouin, S.; Tosin, M.; Murphy, P. V.; Gabius, H. J. *Org. Biomol. Chem.* **2009**, *7*, 4715; (j) Leyden, R.; Velasco-Torrijos, R.; André, S.; Gouin, S. G.; Gabius, H.-J.; Murphy, P. V. *J. Org. Chem.* **2009**, *74*, 9010.

15. See Ref. [12h] and (a) Poláková, M.; Pitt, N.; Tosin, M.; Murphy, P. V. *Angew. Chem., Int. Ed.* **2004**, *43*, 2518; (b) O'Brien, C.; Poláková, M.; Pitt, N.; Tosin, M.; Murphy, P. V. *Chem. Eur. J.* **2007**, *13*, 902.
16. Kjaer, A. *Acta Chem. Scand.* **1948**, *2*, 455.
17. For a related macrocycle derived from phenylenediamine both E and Z amides were observed in an X-ray crystal structure. See: Murphy, P. V.; Müller-Bunz, H.; Velasco-Torrijos, T. *Carbohydr. Res.* **2005**, *340*, 1437.
18. Mohamadi, F.; Richards, N. G. J.; Guida, W. C.; Liskamp, R.; Lipton, M.; Caufield, C.; Chang, G.; Hendrickson, T.; Still, W. C. *J. Comput. Chem.* **1990**, *11*, 440.
19. (a) Leng, F.; Chaires, J. B.; Waring, M. J. *Nucleic Acids Res.* **2003**, *31*, 6191; (b) Shafer, R. H.; Waring, M. J. *Biopolymers* **1980**, *19*, 431; (c) Leroy, J. L.; Gao, X.; Misra, V.; Gueron, M.; Patel, D. J. *Biochemistry* **1992**, *31*, 1407; (d) Fox, K. R.; Gauvreau, D.; Goodwin, D. C.; Waring, M. J. *Biochem. J.* **1980**, *191*, 729; (e) Cornish, A.; Fox, K. R.; Waring, M. J. *Antimicrob. Agents Chemother.* **1983**, *23*, 221; (f) Wakelin, L. P. G.; Waring, M. J. *Biochem. J.* **1976**, *157*, 721.
20. Nygren, J.; Svanvik, N.; Kubista, M. *Biopolymers* **1998**, *46*, 39.
21. The UV spectra are provided in Supplementary data.
22. (a) Deligeorgiev, T. G.; Gadjev, N. I.; Drexhage, K.-H.; Sabnis, R. W. *Dyes and Pigments* **1995**, *29*, 315; (b) Harriman, W. D.; Wabl, M. *Anal. Biochem.* **1995**, *228*, 336.
23. (a) McGhee, J. D. *Biopolymers* **1976**, *15*, 1345; (b) Bonjean, K.; De Pauw-Gillet, M. C.; Defresne, M. P.; Colson, P.; Houssier, C.; Dassonneville, L.; Bailly, C.; Greimers, R.; Wright, C.; Quetin-Leclercq, J.; Tits, M.; Angenot, L. *Biochemistry* **1998**, *37*, 5136; (c) Zhong, W.; Yu, J.-S.; Liang, Y.; Fan, K.; Lai, L. *Spectrochim. Acta, Part A Mol. Biomol. Spectrosc.* **2004**, *60*, 2985; (d) Chaires, J. B.; Dattagupta, N.; Crothers, D. M. *Biochemistry* **1982**, *21*, 3933.
24. Krieger, E.; Darden, T.; Nabuurs, S.; Finkelstein, A.; Vriend, G. *Proteins* **2004**, *57*, 678.
25. Duan, Y.; Wu, C.; Chowdhury, S.; Lee, M. C.; Xiong, G.; Zhang, W.; Yang, R.; Cieplak, P.; Luo, R.; Lee, T. *J. Comput. Chem.* **2003**, *24*, 1999.
26. Page, S. E.; Flood, A.; Gordon, K. C. *J. Chem. Soc., Dalton Trans.* **2002**, *6*, 1180.